ECT* nuclear physics workshop “Light clusters in nuclei and nuclear matter:
Nuclear structure and decay, heavy ion collisions, and astrophysics

ECT* WORKSHOP 2019

Microscopic Description of Multi-clusters in Light Nuclei

Bo Zhou

Hokkaido University

2019/09/04@ECT*

Outline

1. The THSR wave function and Container picture

2. 2D container of α particles in 3^- and 4^- states of ^{12}C

3. Real-Time Evolution Method for cluster calculations

4. Summary and Prospect

VOLUME 87, NUMBER 19 PHYSICAL REVIEW LETTERS 5 NOVEMBER 2001

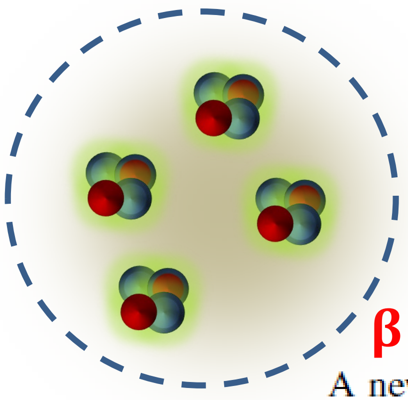

Alpha Cluster Condensation in ^{12}C and ^{16}O

A. Tohsaki,[1] H. Horiuchi,[2] P. Schuck,[3] and G. Röpke[4]
[1]*Department of Fine Materials Engineering, Shinshu University, Ueda 386-8567, Japan*
[2]*Department of Physics, Kyoto University, Kyoto 606-8502, Japan*
[3]*Institut de Physique Nucléaire, F-91406 Orsay Cedex, France*
[4]*FB Physik, Universität Rostock, D-18051 Rostock, Germany*
(Received 29 June 2001; published 17 October 2001)

THSR wave function

A new α-cluster wave function is proposed which is of the α-particle condensate type. Applications to ^{12}C and ^{16}O show that states of low density close to the 3 and 4 α-particle thresholds in both nuclei are possibly of this kind. It is conjectured that all self-conjugate $4n$ nuclei may show similar features.

$$\Phi^{\mathrm{THSR}}(\beta) = \int d^3R_1 \ldots d^3R_n \,\mathrm{Exp}\left[-\frac{R_1^2+\ldots+R_n^2}{\beta^2}\right] \Phi^{\mathrm{Brink}}(R_1, \ldots, R_n)$$

$$\propto \phi_G\, \mathcal{A}\left\{\prod_{i=1}^{n}\left[\mathrm{Exp}\left(-\frac{2(X_i - X_G)^2}{B^2}\right)\phi(\alpha_i)\right]\right\}$$

$$\phi(\alpha) \propto \exp\left[-\sum_{1\le i<j\le 4}(r_i-r_j)^2/(8b^2)\right]$$

β can be considered as the size parameter of the nucleus

$$B^2 = b^2 + 2\beta^2$$

In the past almost 20 years,

✓ The alpha condensation concept
Tohsaki et al., Rev. Mod. Phys. 89, 011002 (2017).

✓ Container picture for general cluster states

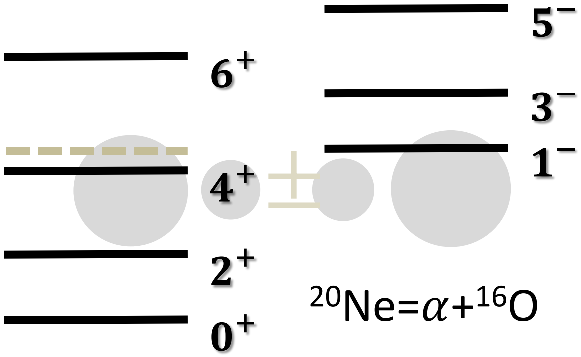

Inversion doublet rotational bands in ^{20}Ne

H Horiuchi and K Ikeda PTP**40** 277(1968)

Container picture for the clusters motion

The clusters make the localized motion confined by the inter-cluster distance parameter *S*.

$$\mathcal{A}\{\exp[-\frac{8\,(\boldsymbol{X}_{\rm rel}-\boldsymbol{S})^2}{5\boldsymbol{b}^2}]\phi(\alpha)\phi(^{16}{\rm O})\}$$

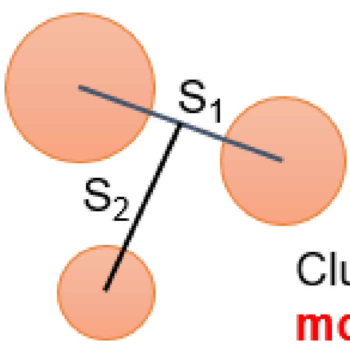

S_1 and S_2: inter-cluster distance parameters.

Clusters make the **localised motions** around the fixed positions.

Traditional cluster model

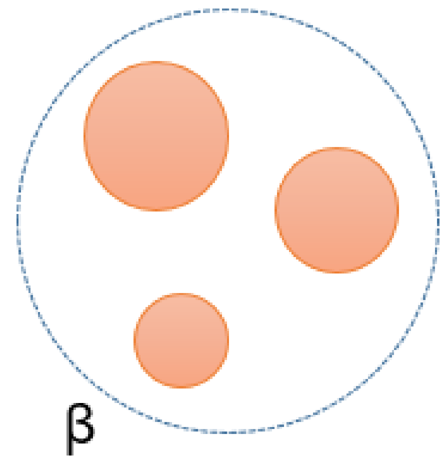

β: the size of the nucleus parameter.

Clusters move around in the **cluster-type mean field**.

Container model

Single THSR wave function≈Superposed Brink wave functions

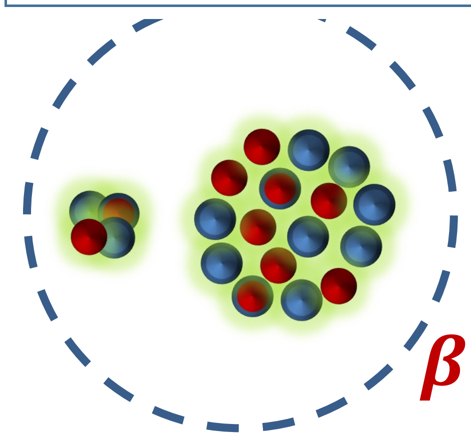

Container picture

The clusters make the nonlocalized motion in a container whose size is described by parameter *β*

$$\mathcal{A}\{\exp[-\frac{8\,X_{\rm rel}{}^2}{5(\boldsymbol{b}^2+2\boldsymbol{\beta}^2)}]\phi(\alpha)\phi(^{16}{\rm O})\}$$

B. Zhou,Y. Funaki,H.Horiuch,Zz. Ren, et al., PRL**110**(2013), PRC**89** (2014).

Rich cluster structures of 0^+ states in ^{12}C

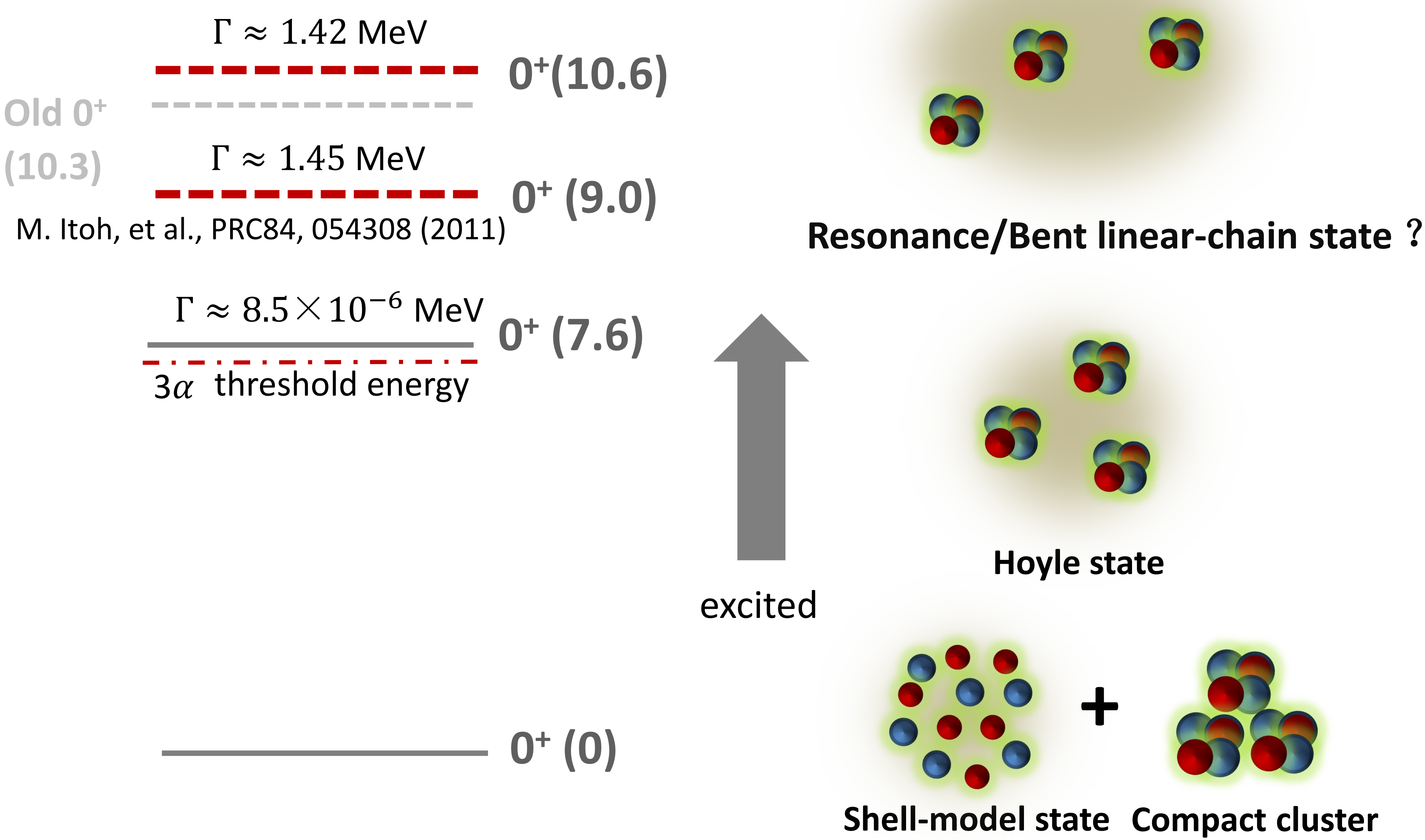

OCM_K : C. Kurokawa and K. Kato, PRC 71, 021301(2005); NPA 792, 87 (2007).

OCM_o : S. Ohtsubo, Y. Fukushima, M. Kamimura, and E. Hiyama,PTEP, 2013, 073D02.

Extended 2α+α THSR Wave Function

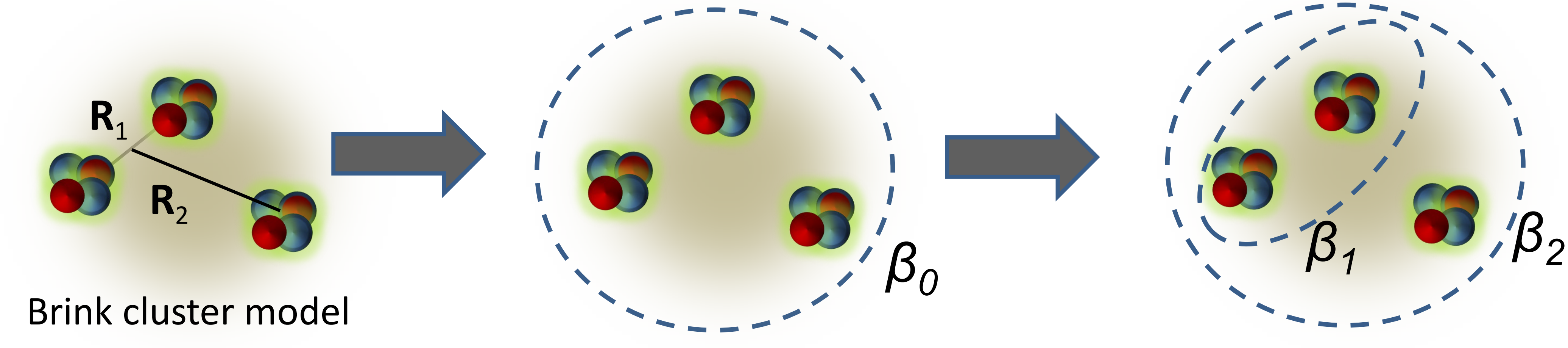

B.Zhou, et al.,PTEP.2014,101D01.

$$\Phi^B(\boldsymbol{R}_1,\boldsymbol{R}_2) \propto \phi_G \mathcal{A}\{\exp(-\frac{(\boldsymbol{r}_1-\boldsymbol{R}_1)^2}{b^2}-\frac{(\boldsymbol{r}_2-\boldsymbol{R}_2)^2}{\frac{3}{4}b^2})\phi(\alpha_1)\phi(\alpha_2)\phi(\alpha_3)\}$$

$$\Phi(\boldsymbol{\beta}_1,\boldsymbol{\beta}_2) = \int d^3R_1 d^3R_2 \exp[-\sum_{i=1}^{2}(\frac{R_{ix}^2}{\beta_{ix}^2}+\frac{R_{iy}^2}{\beta_{iy}^2}+\frac{R_{iz}^2}{\beta_{iz}^2})]\Phi^B(\boldsymbol{R}_1,\boldsymbol{R}_2)$$

$$\propto \phi_G \mathcal{A}\{\exp[-\sum_{i=1}^{2}(\frac{r_{ix}^2}{B_{ix}^2}+\frac{r_{iy}^2}{B_{iy}^2}+\frac{r_{iz}^2}{B_{iz}^2})]\phi(\alpha_1)\phi(\alpha_2)\phi(\alpha_3)\}$$

$$B_{1k}^2 = b^2+\beta_{1k}^2,\ B_{2k}^2 = \frac{3}{4}b^2+\beta_{2k}^2$$

Effective nucleon-nucleon interaction: $V_N = \sum_{i>j}\{(1-M)-MP_\sigma P_\tau\}_{ij}\sum_{n=1}^{2}v_n e^{-\frac{r_{ij}^2}{a_n^2}}.$

Radius-Constraint Method for removing the continuum states.

Y. Funaki, et al., Prog.Theor.Phys.115,115(2006).

The 0_3^+ and 0_4^+ states of ^{12}C

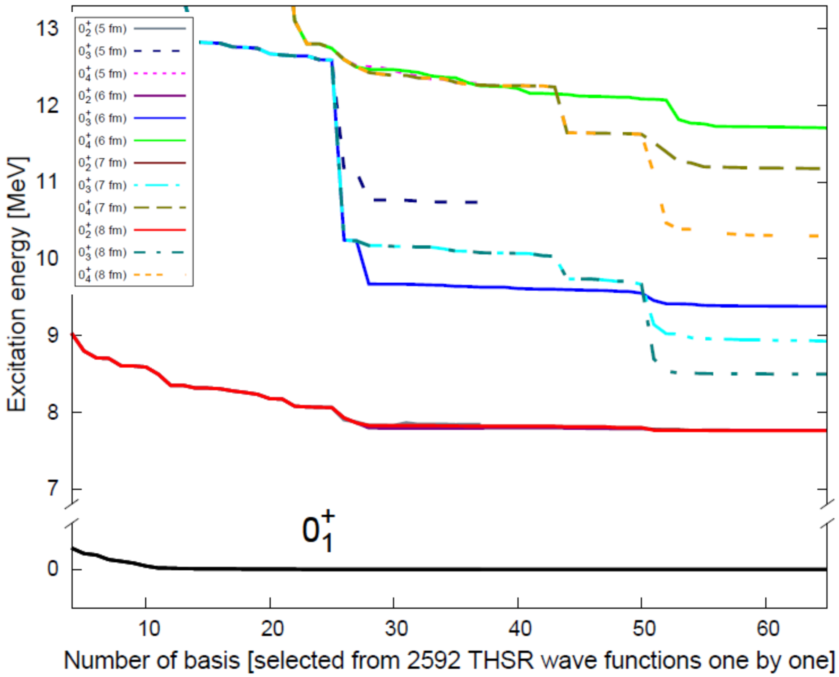

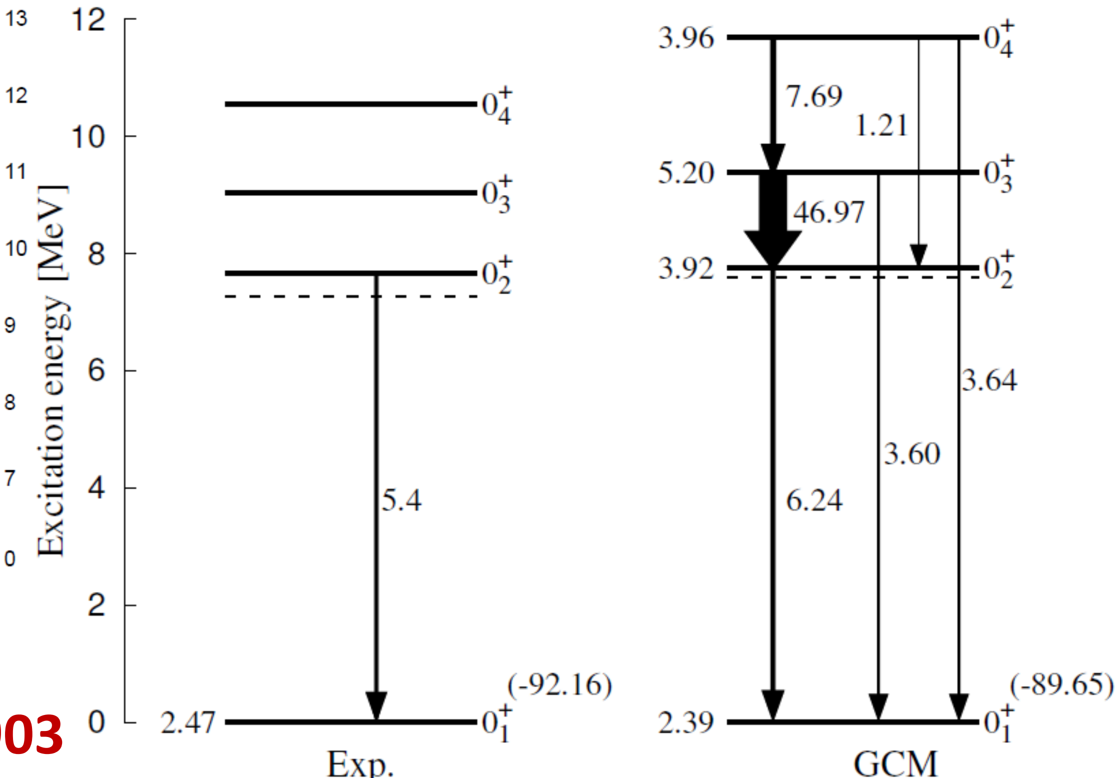

$$|\langle\hat{\Phi}^{0_3^+}_{\rm min1}(\beta_1=6.4,\beta_2=3.0)|\hat{\Phi}^{0_3^+}_{\rm gcm}\rangle|^2$$ = **0.903**

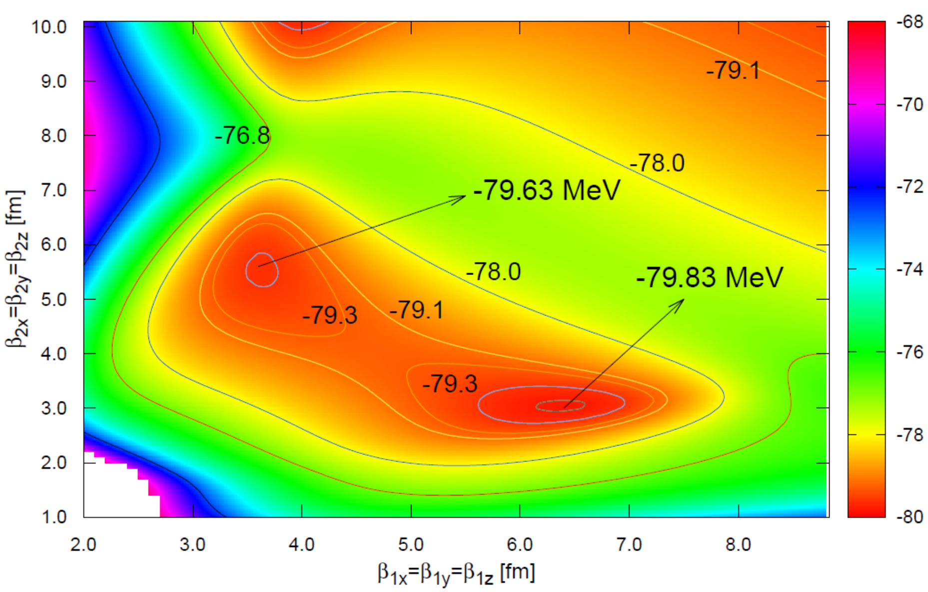

$$P_2^{\perp}=1-n_1|\hat{\Phi}^{0_1^+}\rangle\langle\hat{\Phi}^{0_1^+}|-n_2|\hat{\Phi}^{0_2^+}\rangle\langle\hat{\Phi}^{0_2^+}|,$$

The existence of the 0_3^+ state was confirmed in two ways.

Very large radius, strong monopole transitions between the 0_3^+ state and the Hoyle sate.

B. Zhou, A. Tohsaki, H. Horiuchi, and Z. Ren, PRC**94**, 044319 (2016).

Why do we study the negative-parity states in ^{12}C ?

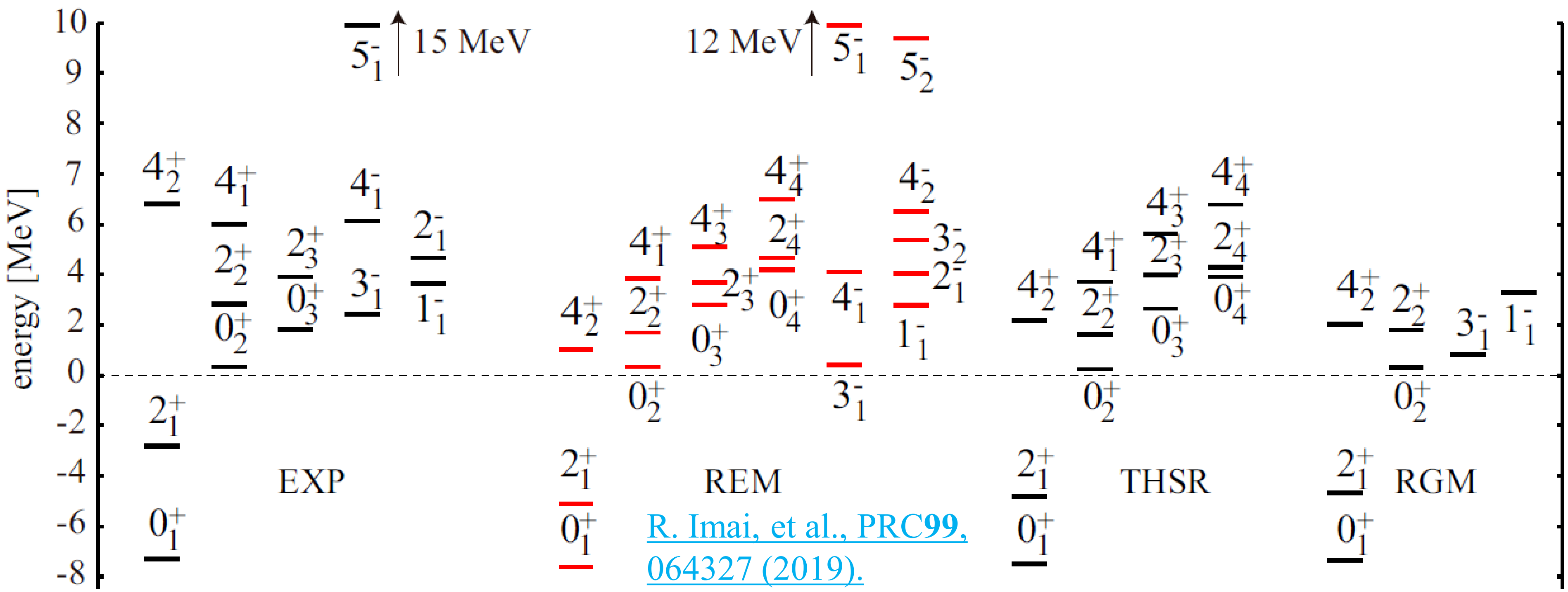

R. Imai, et al., PRC**99**, 064327 (2019).

◎ **A geometrical arrangement picture** of the three alpha particles was proposed.

in terms of representations of unitary algebras

R. Bijker and F. Iachello,PRC**61**, 067305(2000)
R. Bijker and F. Iachello,PRL**112**,152501 (4α) (2014)
D. J. Marín-Lámbarri,et al.,PRL**113**,012502 (2014)

D_{3h} symmetry assumption

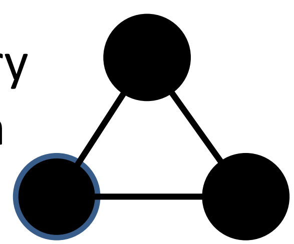

The energy level was reproduced. [0^+, 2^+, 3^-, $4^{\mp}$, 5^-]

◎ **Intrinsic density** from shell model

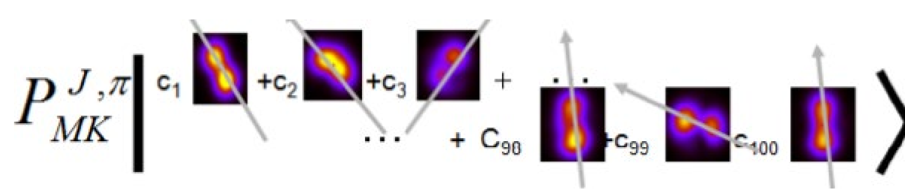

Univ. of Tokyo Group

◎ **Reconstructing transition density**, 3α clustering triangle shape appears (Kimura's talk)

Why do we study the negative-parity states in ^{12}C ?

Recent years, many cluster states have been described quite well by **single THSR wave functions**.

	^{8}Be	^{12}C	^{20}Ne
0^+	1.000(1.8, 7.8)	0_1^+:0.93(1.5, 1.5) (0_1^+:0.978)[a] 0_2^+:0.993(5.3, 1.5)	0.993(0.9, 2.5)
2^+			0.988(0.0, 2.2)
4^+			0.978(0.0, 1.8)
3^-			1.000(3.7, 1.4) 0.999(3.7, 0.0)

Y. Funaki, et al., Prog. Part. Nucl. Phys. **82**, 78 (2015).

PHYSICAL REVIEW C **99**, 051303(R) (2019)

Rapid Communications

Nonlocalized motion in a two-dimensional container of α particles in 3^- and 4^- states of ^{12}C

Bo Zhou,[1,2] Yasuro Funaki,[3] Hisashi Horiuchi,[4] Masaaki Kimura,[2,5] Zhongzhou Ren,[6] Gerd Röpke,[7] Peter Schuck,[8] Akihiro Tohsaki,[4] Chang Xu,[9] and Taiichi Yamada[10]

We want to try to construct a single THSR-type wave function describing exactly the negative-parity sates of ^{12}C.

Container picture for negative-parity states in ^{12}C

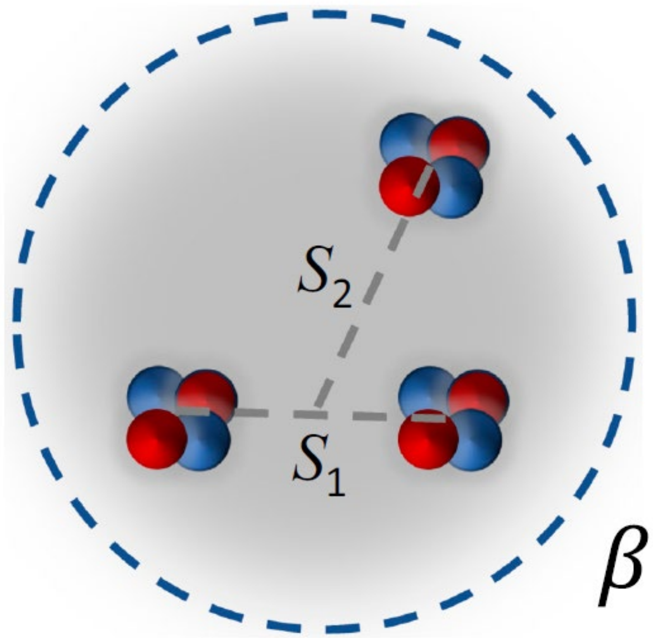

Effective nucleon-nucleon interaction:

$$V_N = \sum_{i>j}\{(1-M) - MP_\sigma P_\tau\}_{ij} \sum_{n=1}^{2} v_n e^{-\frac{r_{ij}^2}{a_n^2}}.$$

Kamimura *et al*. RGM, {Volkov2,*M*=0.59,*b*=1.35 fm}

Nucl. Phys. A351, 456, 1981.

$$\Phi(\boldsymbol{\beta}, \boldsymbol{S}_1, \boldsymbol{S}_2) = \int d^3R_1 d^3R_2 \exp[-\frac{(\boldsymbol{R}_1-\boldsymbol{S}_1)^2}{2\boldsymbol{\beta}^2} - \frac{2(\boldsymbol{R}_2-\boldsymbol{S}_2)^2}{3\boldsymbol{\beta}^2}]\Phi^B(\boldsymbol{R}_1, \boldsymbol{R}_2)$$

$$\propto \phi_G \mathcal{A}\{\exp[-\frac{(\boldsymbol{\xi}_1-\boldsymbol{S}_1)^2}{b^2+2\boldsymbol{\beta}^2} - \frac{(\boldsymbol{\xi}_2-\boldsymbol{S}_2)^2}{3/4\ (b^2+2\boldsymbol{\beta}^2)}]\phi(\alpha_1)\phi(\alpha_2)\phi(\alpha_3)\},$$

$$\Phi^B(\boldsymbol{R}_1, \boldsymbol{R}_2) \propto \phi_G \mathcal{A}\{\exp(-\frac{(\boldsymbol{\xi}_1-\boldsymbol{R}_1)^2}{b^2} - \frac{(\boldsymbol{\xi}_2-\boldsymbol{R}_2)^2}{3/4\ b^2})\phi(\alpha_1)\phi(\alpha_2)\phi(\alpha_3)\},$$

$$\boldsymbol{\xi}_1 = \boldsymbol{X}_2 - \boldsymbol{X}_1 \qquad \boldsymbol{\xi}_2 = \boldsymbol{X}_3 - (\boldsymbol{X}_1 + \boldsymbol{X}_2)/2$$

Variational calculations for the projected 3^- THSR wave function

$$\boldsymbol{S}_1 = (S,0,0),\ \boldsymbol{S}_2 = (0,\sqrt{3}/2S,0) \qquad S=0.5\ \text{fm}.$$

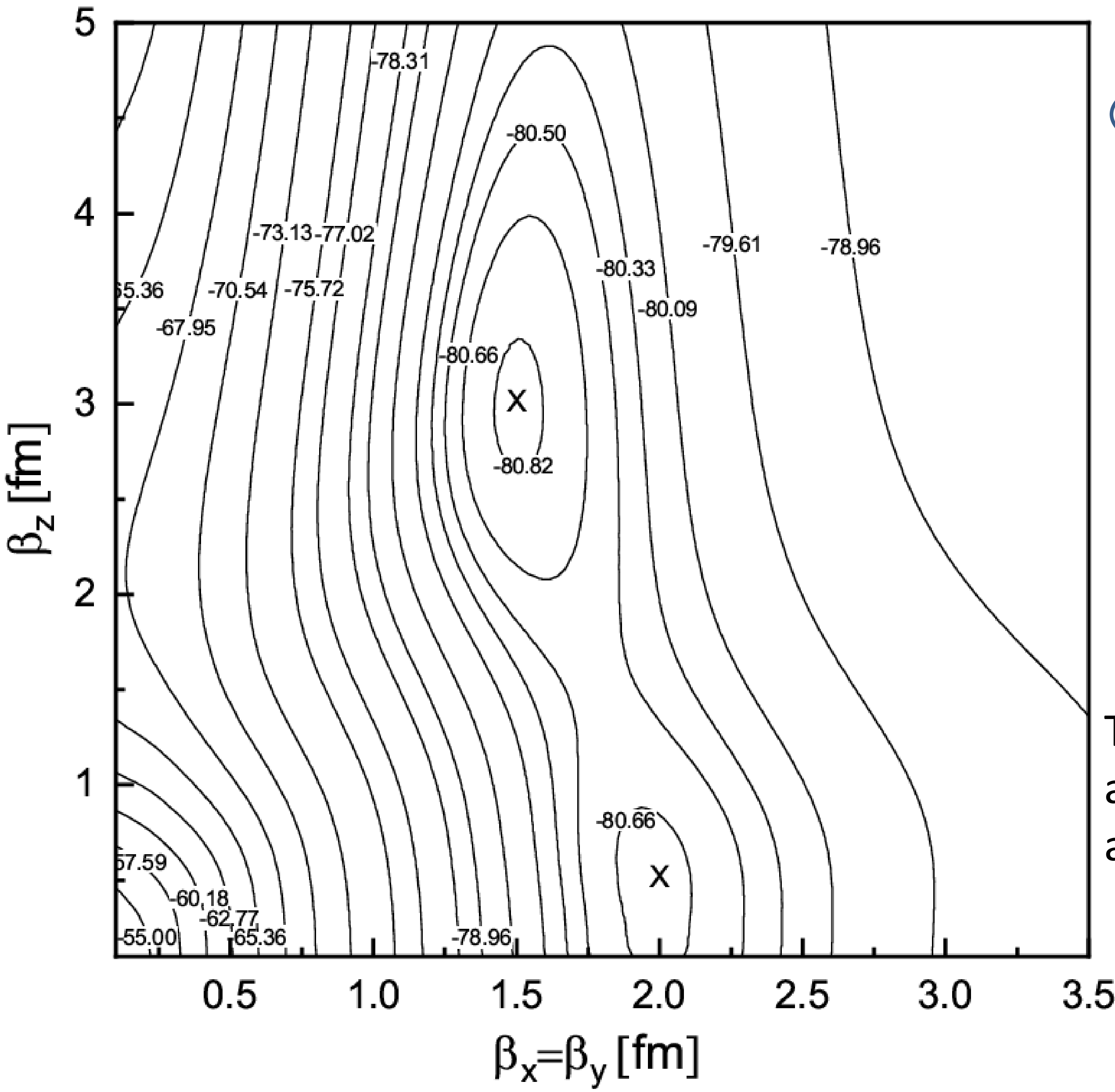

$\boldsymbol{P}^{3-}\Phi$(βx=βy, βz, S=0.5 fm)

Two local minimum points appear in a valley in the contour plot.

$\mathbf{E_1}$(βx=βy=1.5, βz=3.0)=-80.85 MeV

$\mathbf{E_2}$(βx=βy=2.0, βz=0.5)=-80.78 MeV

The two optimum wave functions are very close after the parity and angular momentum projections.

$|\langle \Phi_1^{3-} | \Phi_2^{3-} \rangle|^2 = 0.98$

Variational calculations for the projected 4^- THSR wave function

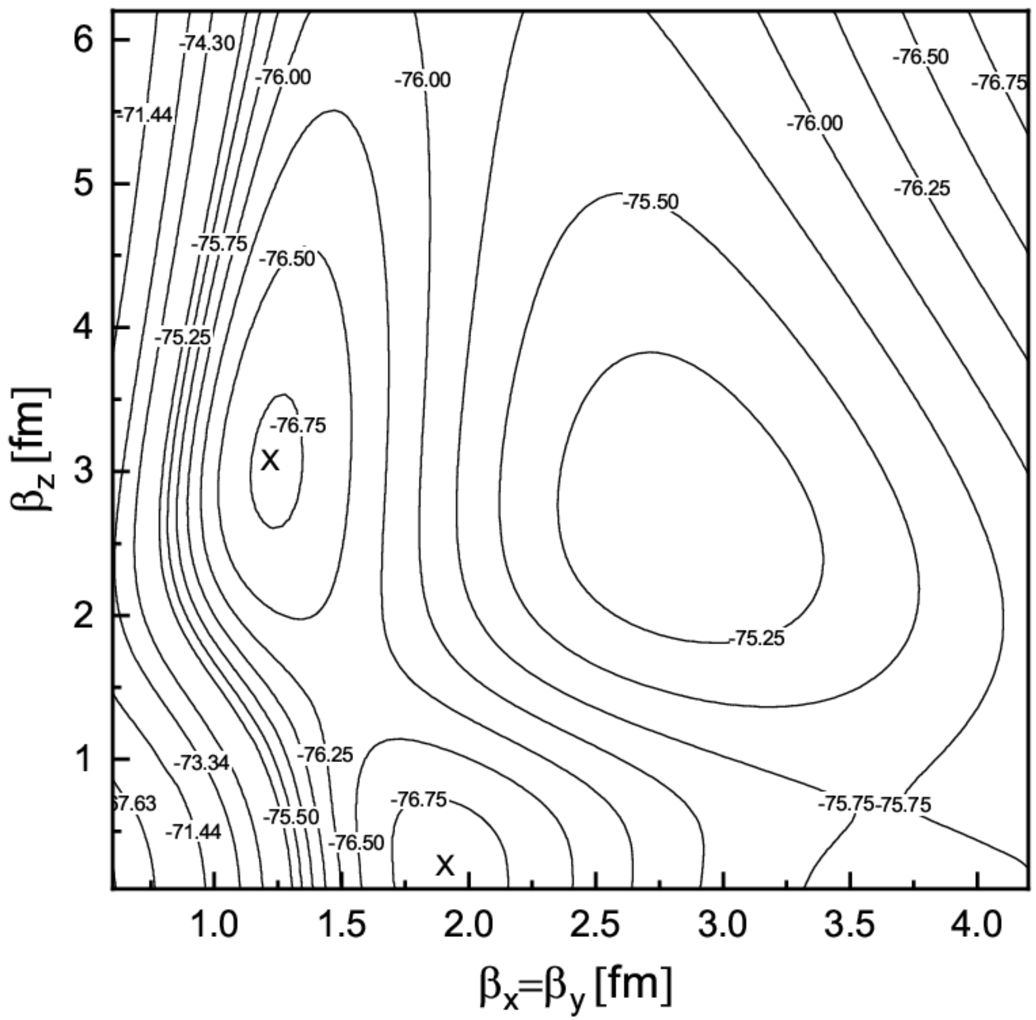

$\boldsymbol{P}^{4-}\Phi$(βx=βy, βz, S=0.5 fm)

Two local minimum points appear in a valley in the contour plot.

$\mathbf{E}_1$(βx=βy=1.9, βz=0.2)=-76.87 MeV

$\mathbf{E}_2$(βx=βy=1.2, βz=3.0)=-76.79 MeV

The two optimum wave functions are very close after the parity and angular momentum projections.

$|\langle\boldsymbol{\Phi}_1^{4-}|\boldsymbol{\Phi}_2^{4-}\rangle|^2$ **=0.98**

Jpi	βx=βy	βz	Min.Eng
3^-	1.5	3	-80.85
3^-	**2**	**0.5**	-80.70
4^-	**1.9**	**0.2**	-76.87
4^-	1.2	3	-76.79

The **similar intrinsic cluster structure** is suggested for the 3^- and 4^- states.

GCM Brink calculations for the 3^- and 4^- states

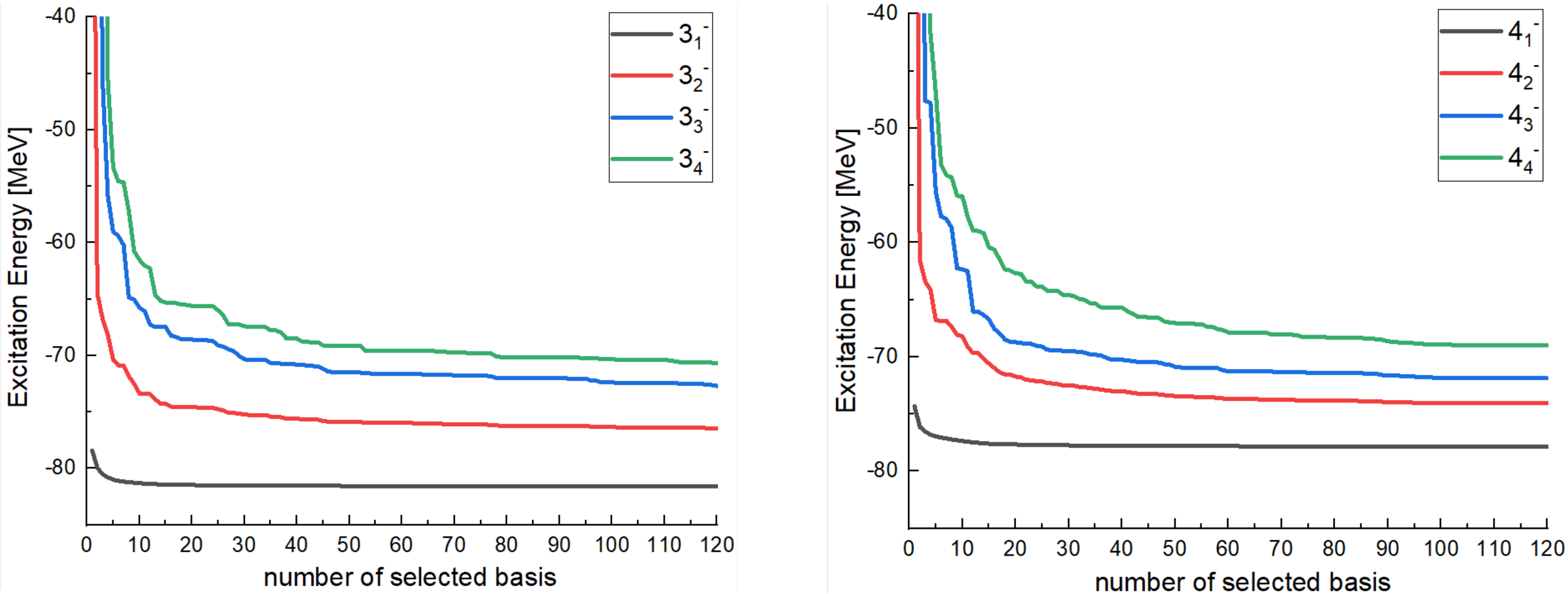

◎ We mainly focus on the first 3^- and 4^- states in the GCM calculations.

◎ The “intrinsic shape” is difficult to be extracted from the superposed wave functions.

Nonlocalized motion for 3α clusters in ^{12}C

$$\propto \mathcal{A}\{\exp[-\frac{(\boldsymbol{\xi}_1-\boldsymbol{S}_1)^2}{b^2+2\boldsymbol{\beta}^2}-\frac{(\boldsymbol{\xi}_2-\boldsymbol{S}_2)^2}{3/4\ (b^2+2\boldsymbol{\beta}^2)}]\phi(\alpha_1)\phi(\alpha_2)\phi(\alpha_3)\}$$

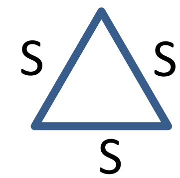

$$\boldsymbol{S}_1=(S,0,0),\ \boldsymbol{S}_2=(0,\sqrt{3}/2S,0)$$

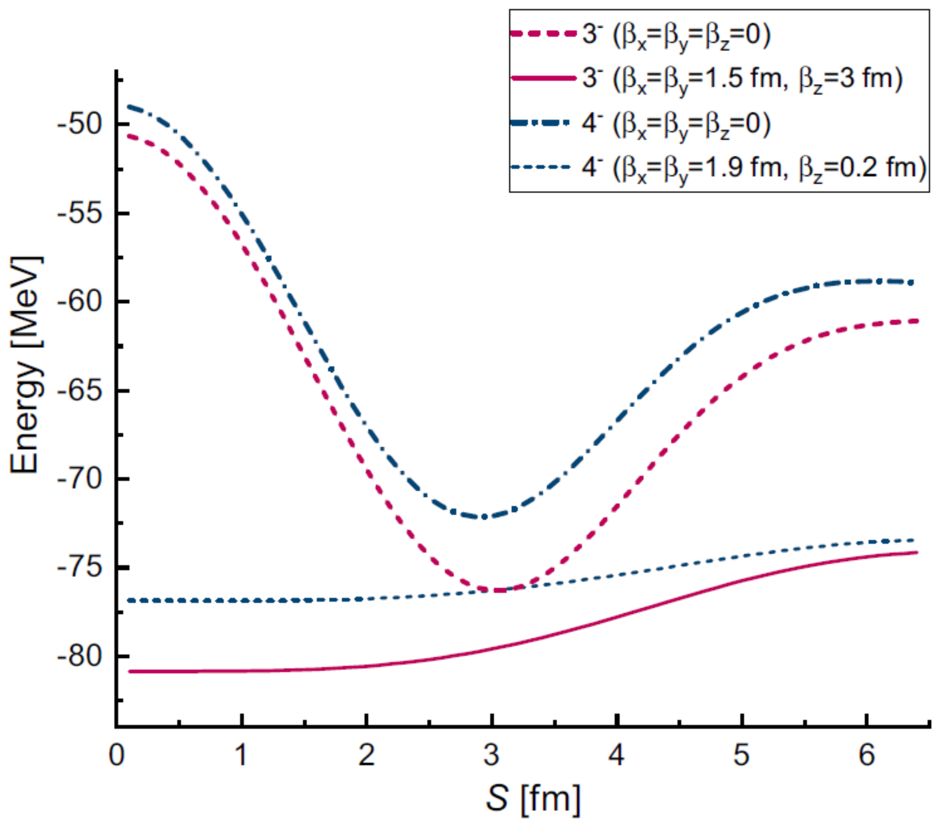

- There are two distinct pockets around 3 fm for the 3$^-$ and 4$^-$ states for Brink wave functions ($\boldsymbol{\beta}$=0).
- If we introduce the width variable of the relative wave function β, we find more deeper energies and S⟶0.
- The obtained single THSR wave functions are almost equivalent to RGM solutions.

TABLE I. Calculated energies from the single optimal THSR wave functions in Eq. (1), the single optimal Brink wave functions in Eq. (2), and the Brink-GCM wave functions for the 3^- and 4^- states. The values of the squared overlap between the single optimal THSR/Brink wave functions and the Brink-GCM wave functions are also shown.

J^π	$E^{\rm Brink}_{\rm min}(\boldsymbol{R}_1,\boldsymbol{R}_2)$	$E^{\rm THSR}_{\rm min}(\boldsymbol{\beta})$	$E^{\rm Brink}_{\rm GCM}$	$\lvert\langle\Phi^{\rm Brink}_{\rm GCM}\lvert\Phi^{\rm Brink}_{\rm min}(\boldsymbol{R}_1,\boldsymbol{R}_2)\rangle\rvert^2$	$\lvert\langle\Phi^{\rm Brink}_{\rm GCM}\lvert\Phi^{\rm THSR}_{\rm min}(\boldsymbol{\beta})\rangle\rvert^2$
3^-	−78.4	−80.9	−81.6	0.78	0.96
4^-	−74.4	−76.9	−77.8	0.72	0.92

Nonlocalized motion for 3α clusters in ^{12}C

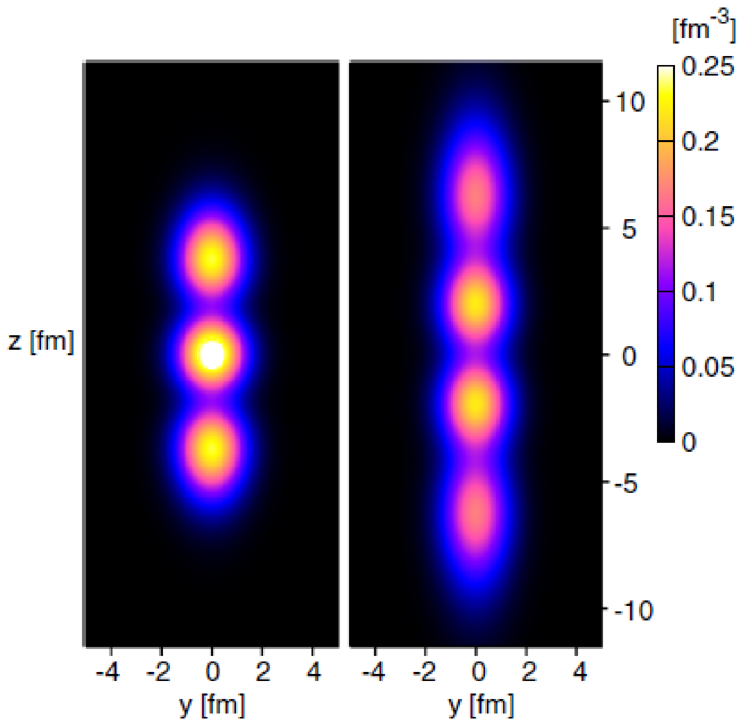

FIG. 3 (color online). Intrinsic density profiles of the 3α- (Left) and 4α- (Right) linear-chain states generated from the THSR wave functions before angular-momentum projection at ($\beta_x = \beta_y = 0.1$ fm, $\beta_z = 5.1$ fm) and ($\beta_x = \beta_y = 0.1$ fm, $\beta_z = 8.2$ fm), respectively.

T.Suhara,et al.,PRL112,062501(2014).

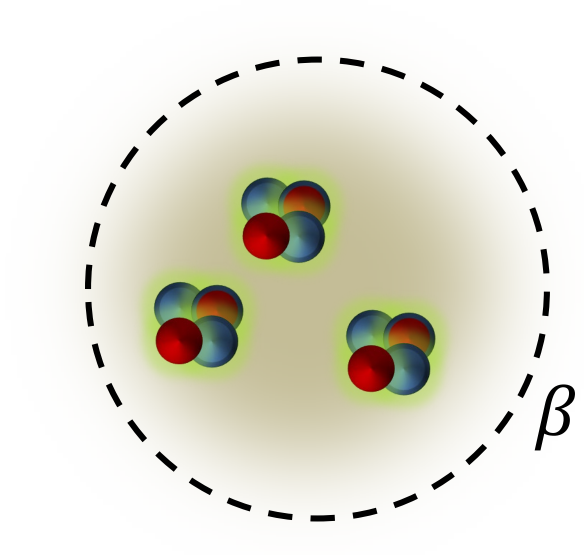

Due to the Pauli principle, an effective localized clustering in the container model was found in the two-cluster ^{20}Ne system and 3α and 4α one-dimensional linear-chain system.

Intrinsic cluster structure for 3α clusters in ^{12}C

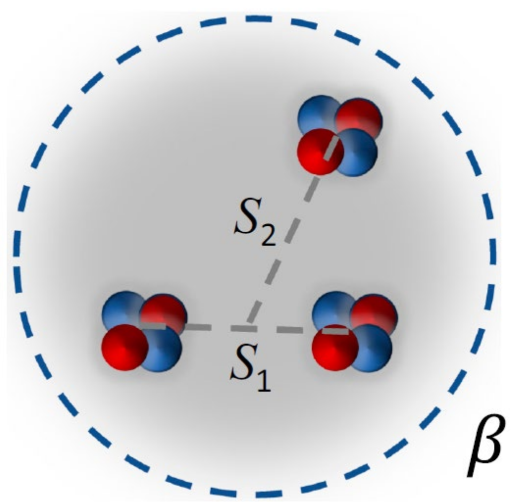

We really obtained the single high-accuracy THSR-type wave functions for 3^- and 4^- states,

$$\propto \mathcal{A}\{\exp[-\frac{(\boldsymbol{\xi}_1-\boldsymbol{S}_1)^2}{b^2+2\boldsymbol{\beta}^2}-\frac{(\boldsymbol{\xi}_2-\boldsymbol{S}_2)^2}{3/4\ (b^2+2\boldsymbol{\beta}^2)}]\phi(\alpha_1)\phi(\alpha_2)\phi(\alpha_3)\}$$

we take $\beta_x=\beta_y$=2.0 fm and β_z=0.5 fm as the size parameters

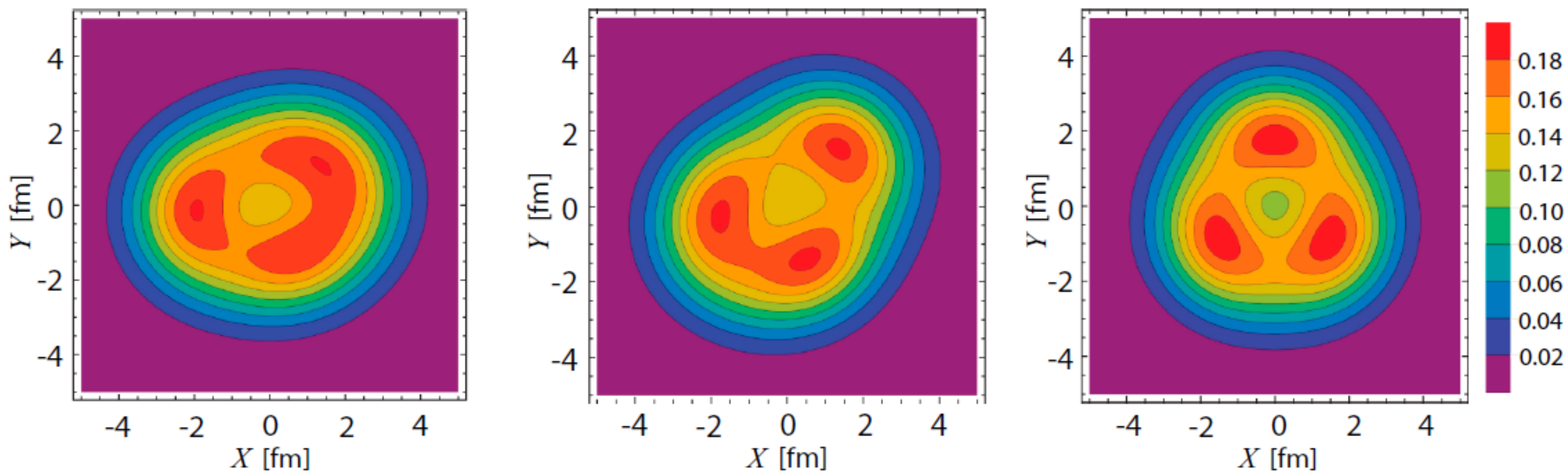

$|\langle\Phi^{3^-}(3/2,3/2,1/2)|\Phi^{3^-}_{\rm GCM}\rangle|^2$=0.94 $|\langle\Phi^{3^-}(1,3/2,3/2)|\Phi^{3^-}_{\rm GCM}\rangle|^2$=0.93 $|\langle\Phi^{3^-}(3/2,0,3/2)|\Phi^{3^-}_{\rm GCM}\rangle|^2$=0.94

$|\langle\Phi^{4^-}(3/2,3/2,1/2)|\Phi^{4^-}_{\rm GCM}\rangle|^2$=0.92 $|\langle\Phi^{4^-}(1,3/2,3/2)|\Phi^{4^-}_{\rm GCM}\rangle|^2$=0.92 $|\langle\Phi^{4^-}(3/2,0,3/2)|\Phi^{4^-}_{\rm GCM}\rangle|^2$=0.92

B. Zhou, et al., Phys. Rev. C **99**, 051303(R) (2019).

The extension of the THSR wave function

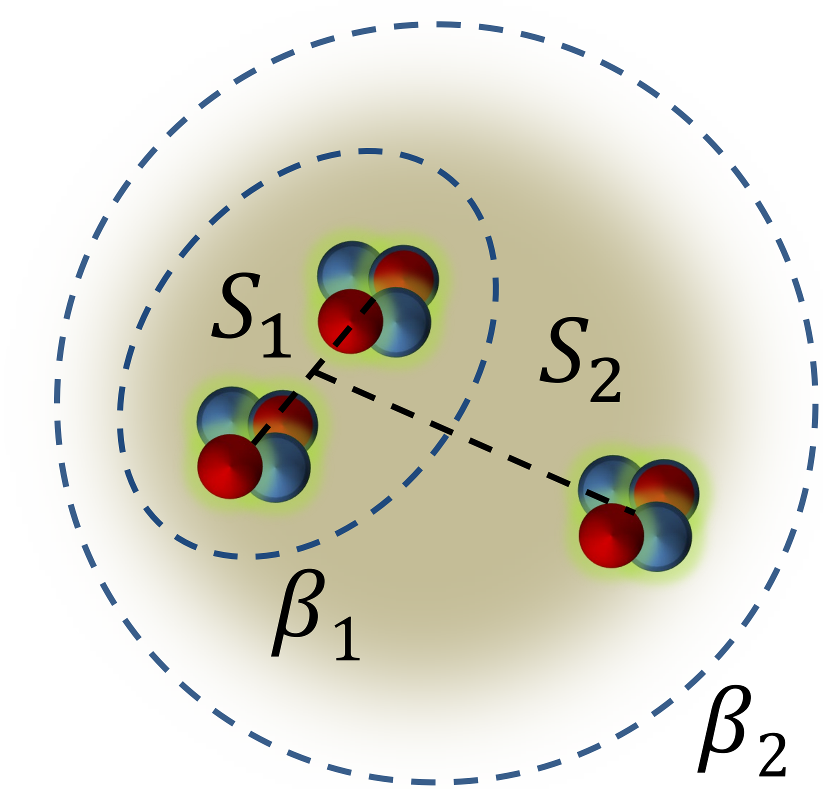

The complete THSR wave function is explicit but has vector parameters

$$\beta \rightarrow (\beta_1, \beta_2, S_1, S_2)$$

Original Complex

- Time-consuming computations
- Picture is not simple enough for explanation

$$\Phi(\boldsymbol{\beta}_1, \boldsymbol{\beta}_2, \boldsymbol{S}_1, \boldsymbol{S}_1) = \int d^3R_1 d^3R_2 \exp[-\frac{(\boldsymbol{R}_1 - \boldsymbol{S}_1)^2}{\beta_1^2} - \frac{(\boldsymbol{R}_2 - \boldsymbol{S}_2)^2}{\beta_2^2}]\Phi^B(\boldsymbol{R}_1, \boldsymbol{R}_2)$$

$$\propto \phi_G \mathcal{A}\{\exp[-\frac{(\boldsymbol{\xi}_1 - \boldsymbol{S}_1)^2}{B_1^2} - \frac{(\boldsymbol{r}_2 - \boldsymbol{S}_2)^2}{B_2^2}]\phi(\alpha_1)\phi(\alpha_2)\phi(\alpha_3)\},$$

$$B_1^2 = b^2 + \boldsymbol{\beta}_1^2,\ B_2^2 = \tfrac{3}{4}b^2 + \boldsymbol{\beta}_2^2.$$

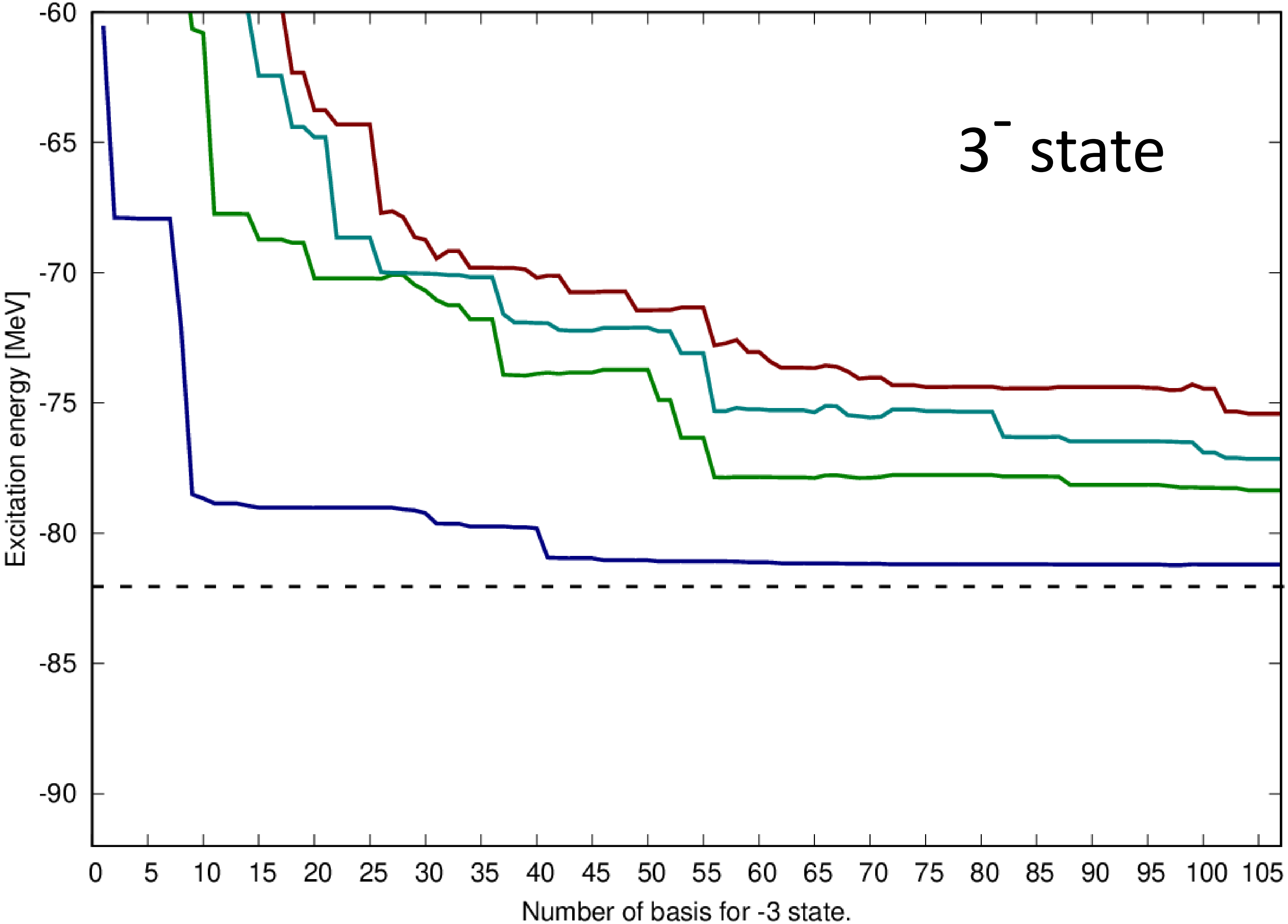

REM	-81.6464	-76.6464		
2D-THSR	-81.2035	-78.3471	-77.1384	-75.4085

(*Preliminary*)

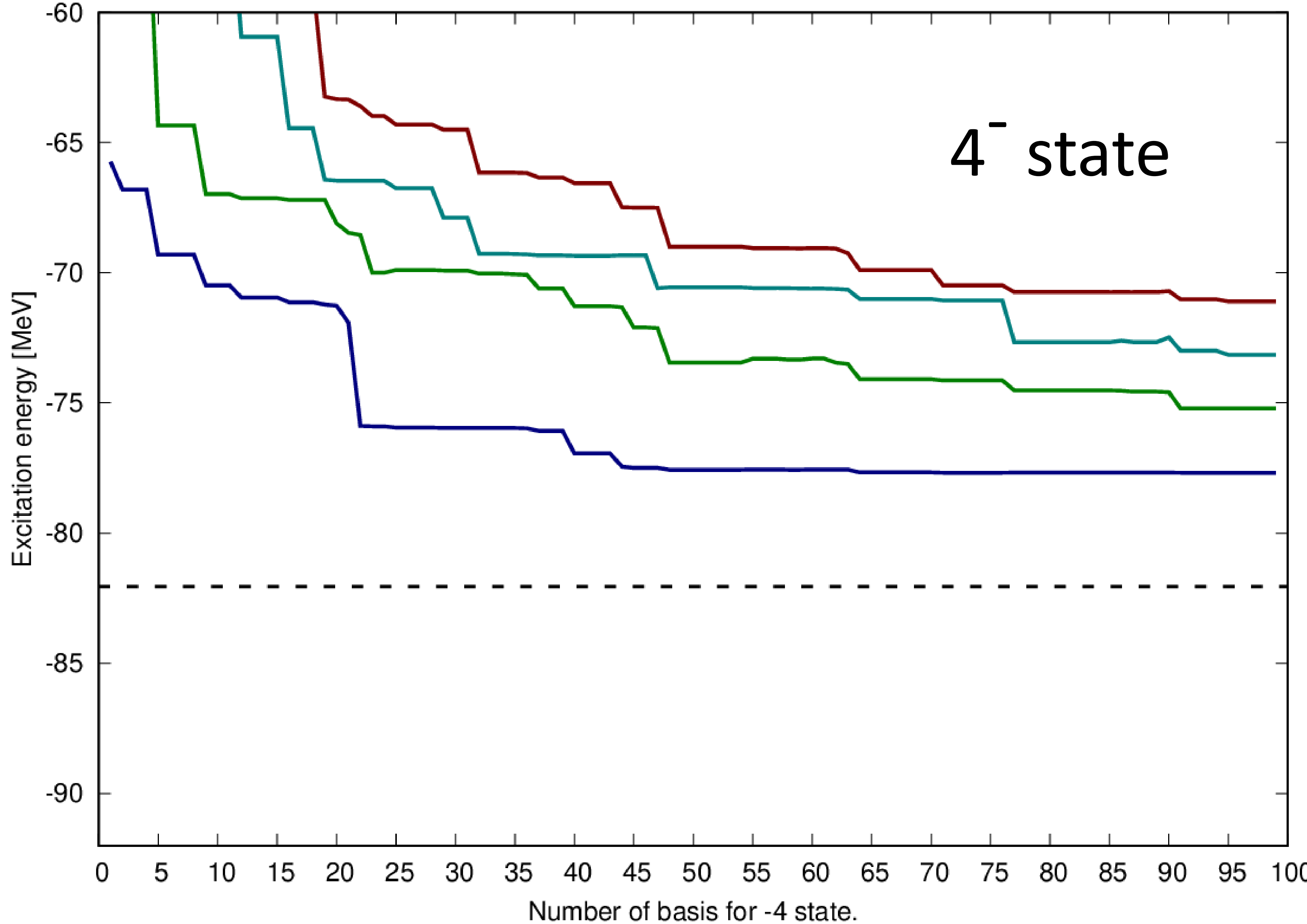

REM	-77.9464	-75.646		
2D-THSR	-77.6791	-75.215	-73.1463	-71.1002

(*Preliminary*)

Recent Real-Time Evolution Method Calculations

from Hokkaido University group

(Kimura, Motoki, Shin, Bo)

$$\Psi = \sum_{n=1}^{N_{max}} c_n \Phi_n$$

Nuclear state (Ψ) — Model wave function (Φ_n)

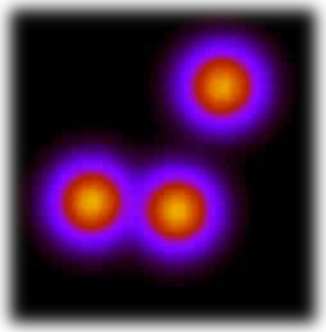

(by Kimura)

Real-Time evolution method

Model wave function (time-dependent wave packets)

○ Slater determinant of nucleon wave packets

$$\Phi(t) = \mathcal{A}\{\,\phi(\boldsymbol{Z}_1(t)), \ldots, \phi(\boldsymbol{Z}_A(t))\,\}$$

$$\phi(\boldsymbol{Z}_i(t)) = \exp\{-\nu(\boldsymbol{r} - \boldsymbol{Z}_i(t))^2\}\,(\alpha_i(t)\,|\uparrow\rangle + \beta_i(t)\,|\downarrow\rangle)$$

○ Dynamical variables of the model (time-dependent parameters)

$\boldsymbol{Z}_i(t)$: Centroids of wave packets (position and momentum)

$\alpha_i(t)\ \beta_i(t)$: Spin directions

$$H = \sum_{i=1}^{A} t(i) - t_{cm} + \sum_{i<j}^{A} v(ij)$$

○ Microscopic Hamiltonian with effective/bara NN interactions

Real-Time evolution method

◎ Time-dependent variational principle

$$\delta \int dt \, \frac{\langle \Phi(t) | i\hbar d/dt - H | \Phi(t) \rangle}{\langle \Phi(t) | \Phi(t) \rangle} = 0$$

◎ Equation of Motion for nucleon wave packets

$$\Rightarrow \quad i\hbar \frac{d\boldsymbol{Z}_i(t)}{dt} = \sum_j C_{ij}^{-1} \frac{\partial \mathcal{H}}{\partial \boldsymbol{Z}_j^*(t)}$$

$$\mathcal{H} = \frac{\langle \Phi(t) | H | \Phi(t) \rangle}{\langle \Phi(t) | \Phi(t) \rangle}, \quad C_{ij} = \frac{\partial^2}{\partial \boldsymbol{Z}_i^* \partial \boldsymbol{Z}_j} \log \langle \Phi(t) | \Phi(t) \rangle$$

^{6}He (6 nucleons)

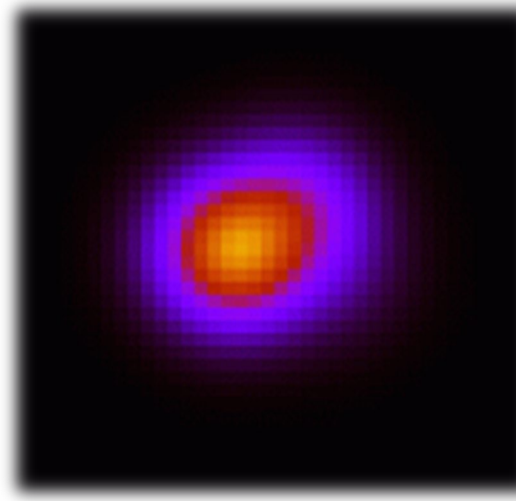

by Kimura

○ By solving EOM, we obtain ensemble of wave functions

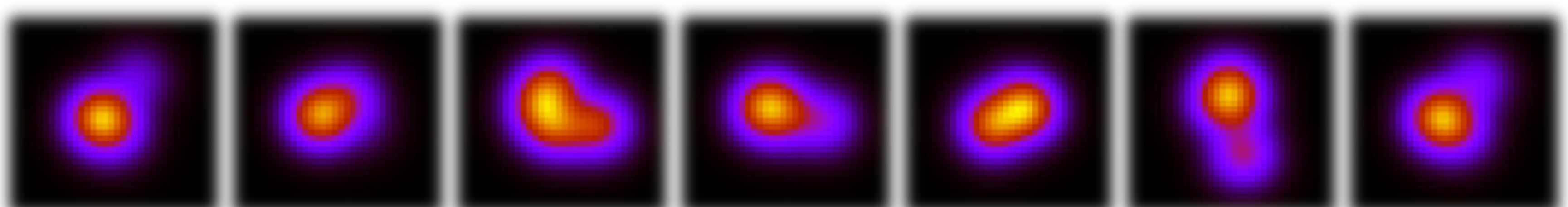

t = 0 fm/c 100 fm/c 200 fm/c 300 fm/c 400 fm/c 500 fm/c 600 fm/c …

Real-Time evolution method

◎ This ensemble has nice properties

J. Schnack and H. Feldmeier, NPA601, 181 (1996).
A. Ono and H. Horiuchi, PRC53, 845 (1996), PRC53, 2341 (1996).

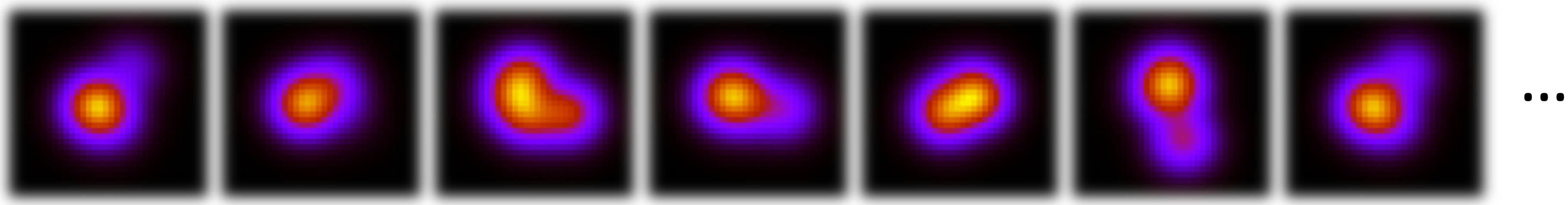

t = 0 fm/c 100 fm/c 200 fm/c 300 fm/c 400 fm/c 500 fm/c 600 fm/c

① The ensemble has ergodicity

All possible quantum states will appear after long-time propagation

② The ensemble follows *quantum* statistics

Important quantum states appear more frequently,
if the excitation energy is properly chosen

From M. Kimura

Real-Time evolution method

◎ We superpose time dependent wave function and diagonalize the Hamiltonian

$\Psi^{J\pi} = f_1$ 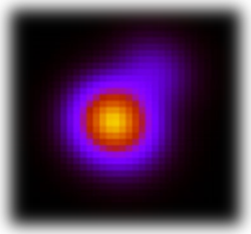 $+ f_2$ 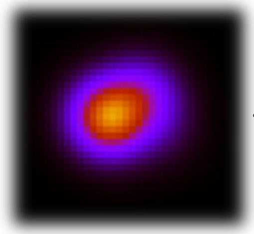 $+ f_3$ 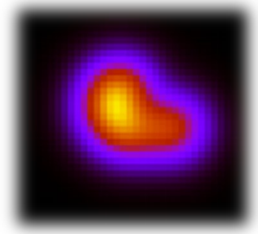 $+ f_4$ 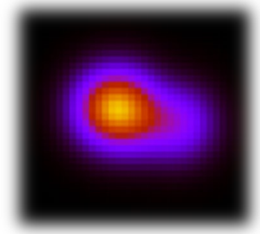 ...

$$= \int_0^{T_{max}} dt \ f(t) \hat{P}^J_{MK} \Phi(t)$$

$f_1, f_2, f_3, f_4, \ldots$ are determined by the diagonalization of Hamiltonian

○ The result (eigen energy & wave function) should be converged after the long-time propagation

○ The result should not depend on the initial condition at t=0

From M. Kimura

Benchmark calculations for few-body systems

From Kimura

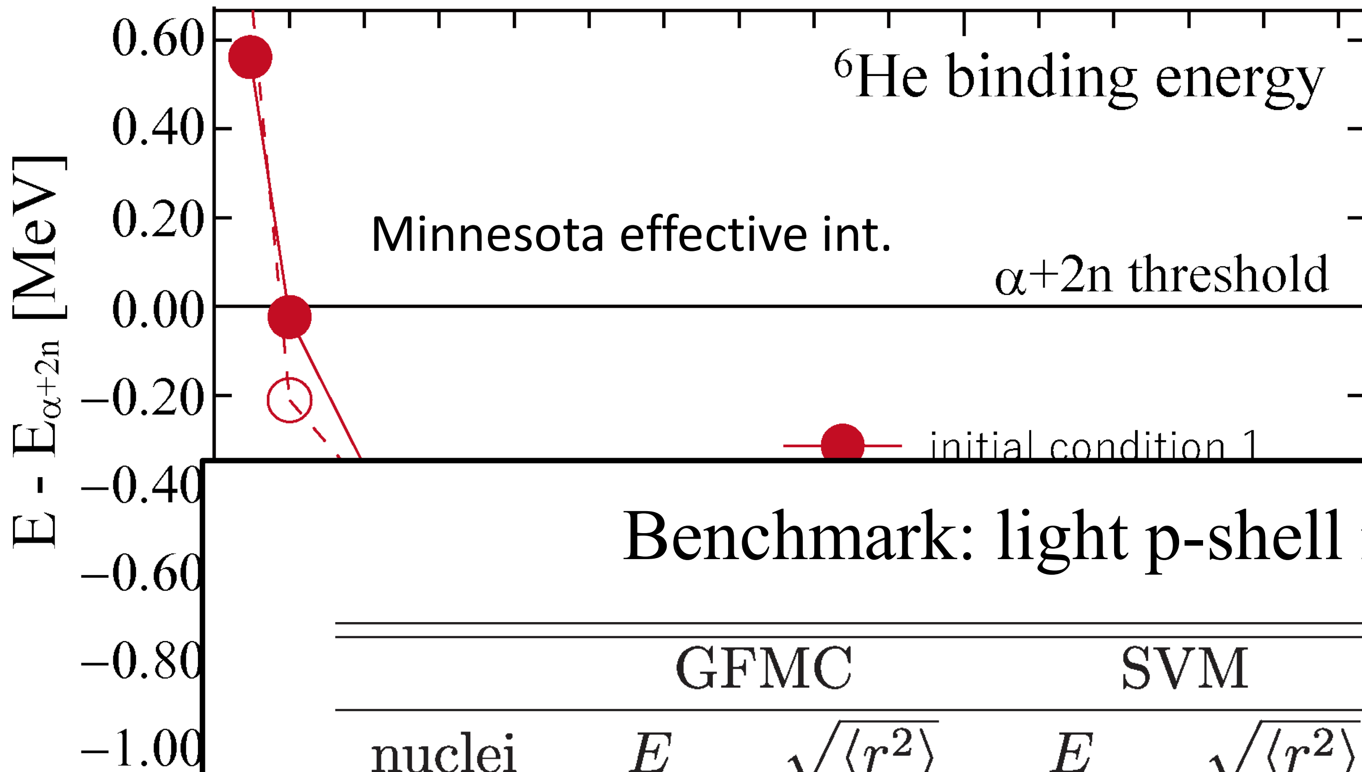

^{6}He (6 nucleons)

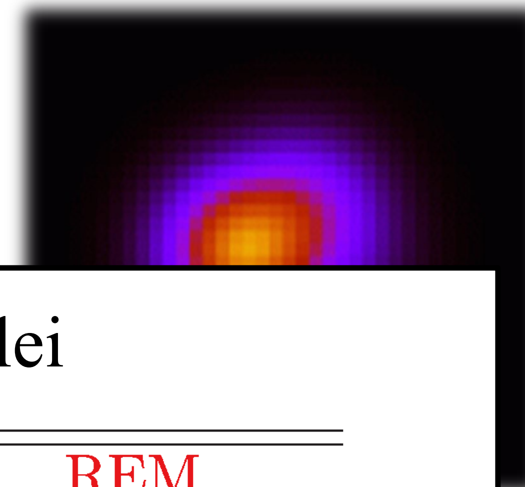

Benchmark: light p-shell nuclei

	GFMC		SVM		REM	
nuclei	E	$\sqrt{\langle r^2 \rangle}$	E	$\sqrt{\langle r^2 \rangle}$	E	$\sqrt{\langle r^2 \rangle}$
^{3}H	-8.26	1.68	-8.25	1.68	-8.25	1.68
^{4}He	-31.3	1.36	-31.4	1.41	-31.4	1.39
^{6}He	-66.3	1.50	-66.3	1.52	-66.3	1.50
^{7}Li	-	-	-83.4	1.68	-83.5	1.67

GFMC: Green function Monte Carlo [2] SVM: Stochastic variational method [8]

* An effective potential "Mulfliet-Tjon potential V (MTV)" was used.

Benchmark calculations for ^{12}C (3α cluster system)

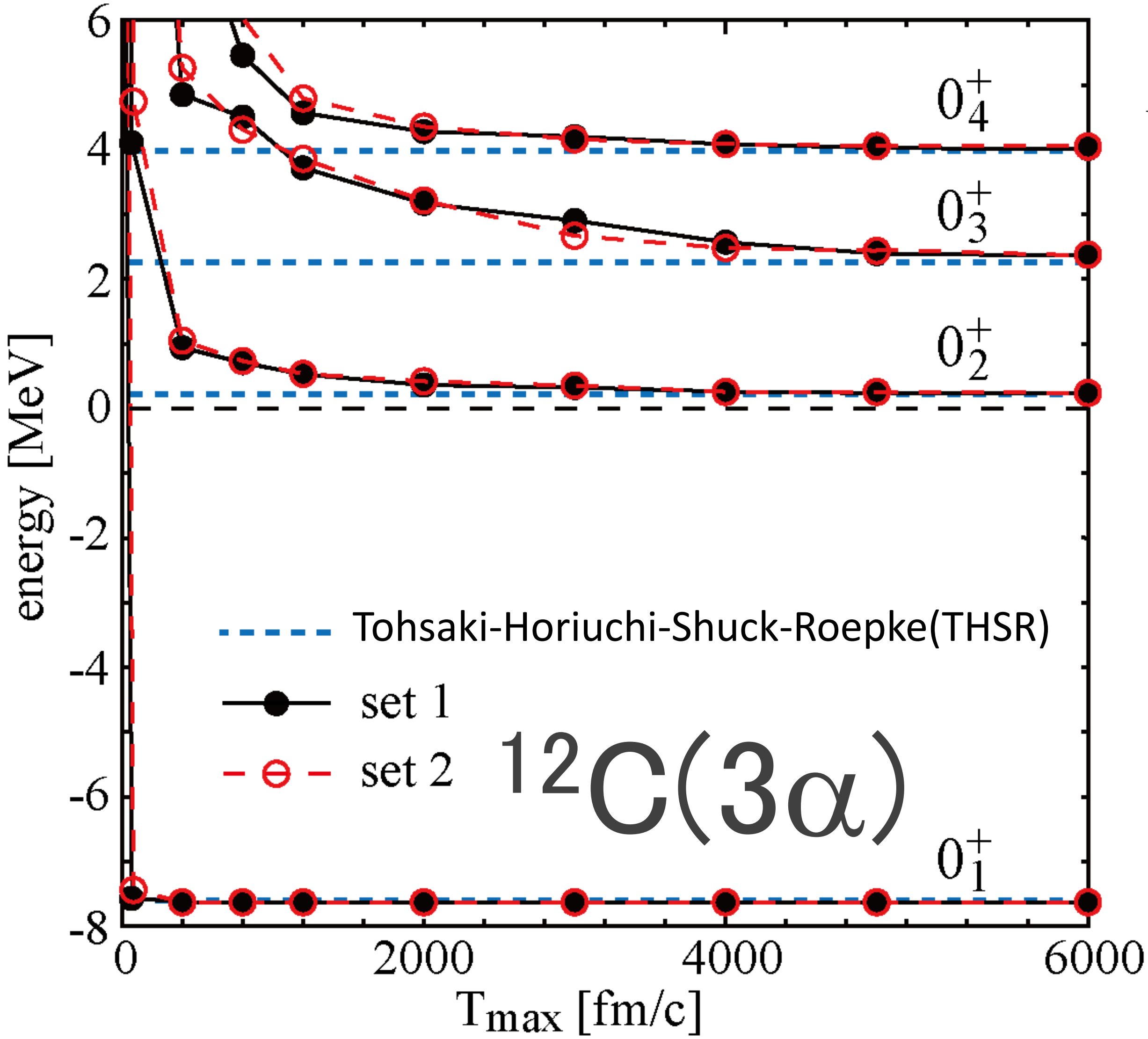

$$\Psi^{J\pi} = \int_0^{T_{max}} dt \;\; f(t) \hat{P}^J_{MK} \Phi(t)$$

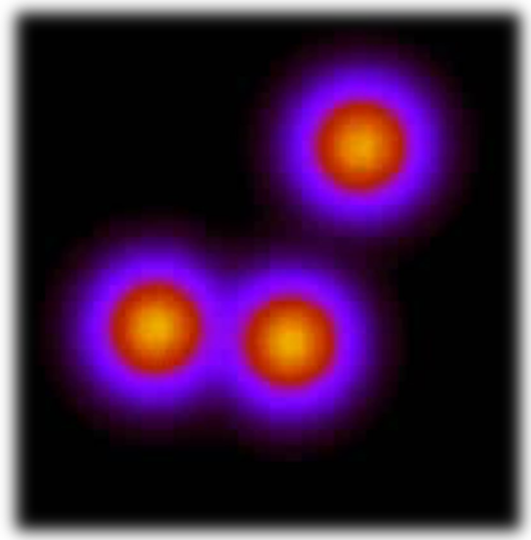

R. Imai, T. Tada, and M. Kimura, Phys. Rev. C **99**, 064327 (2019).

Summary and Prospect

- **The two-dimensional container picture for the ^{12}C**
  The nonlocalized motion of 3^- and 4^- states.
  GCM-THSR calculations for spectrum of ^{12}C

- **The real time-evolution method for nuclear cluster structure**
  AMD as a nucleon wave function calculations in REM (^{6}He)
  Pure Nα cluster wave function calculation in REM (^{16}O)
  Neutron-rich nuclei studies in REM (^{9}Be, ^{10}Be, ^{12}Be, ^{13}C)

Thanks for my collaborators and your attentions !

Yasuro Funaki	(Kanto Gakuin Univ.)
Taiichi Yamada	(Kanto Gakuin Univ.)
Zhongzhou Ren	(Tongji Univ.)
Chang Xu	(Nanjing Univ.)
Qing Zhao	(Nanjing Univ.)
Masaaki Kimura	(Hokkaido Univ.)
Hisashi Horiuchi	(Osaka Univ.)
Akihiro Tohsaki	(Osaka Univ.)
Mengjiao Lyu	(Osaka Univ.)
Gerd Röpke	(Rostock Univ.)
Peter Schuck	(Paris-Sud Univ.)